Wavelet-Alienation-Neural Based Protection Scheme for STATCOM Compensated Transmission Line

Bhuvnesh Rathore, Om Prakash Mahela, *Member, IEEE*, Baseem Khan, *Member, IEEE*, Hassan Haes Alhelou, *Member, IEEE*, and Pierluigi Siano, *Senior Member, IEEE*

***Abstract*—The custom power devices play important role for enhancing the power transfer capacity of transmission system. However, these devices introduce challenges of under-reach or over-reach, in the protection of transmission system. This paper introduces a novel, protection algorithm based on wavelet-alienation-neural technique for STATCOM-compensated transmission system. For detecting and classifying faults, approximate coefficients are computed from the post-fault quarter cycle current waveforms. Fault index, which is summation of Alienation coefficients (computed by approximate coefficients) of both the buses, is computed and compared with the threshold magnitude for detecting and classifying the different faults. For the determination of fault location, Artificial Neural Network (ANN) is applied, with input as three-phase approximate coefficients, evaluated from the voltage and current signals over a time duration of a quarter cycle. Robustness of the developed scheme has been validated for various faults at different locations with varying fault impedances and angles of fault incidence.**

***Index Terms*—Alienation Coefficients, artificial neural network, fault detection and classification, static compensator (STATCOM), Wavelet transform.**

I. Introduction

THE stability and economy of a power system greatly depends upon reliability and efficiency of the transmission networks. In modern power system, capacity of power transfer and quality of power are enhanced by using FACTS devices. Amongst these devices, Static compensator (STATCOM) is one of the shunt compensation devices, used for reactive power management in transmission system. These devices can affect the distance protection scheme both in steady state and transient conditions [1]. Current injection and absorption by the shunt compensators lead to over and under reach of traditional distance relays. Thus, it is a challenge to access correct fault location on the compensated transmission line.

Different protection methodologies have been introduced in the literature for STATCOM-compensated transmission lines. Zhang, *et al.* [2] suggested various modifications to distance relaying for STATCOM compensated transmission lines. Authors in [3]–[5], presented the analytical studies indicating the effects of STATCOM operation on distance relaying. Sidhu, *et al.* [6] illustrated the performance of relays used for distance protection for the shunt compensated transmission lines. Performance comparison of various schemes used for distance protection was reported in [7]. Pilot relaying schemes had been proposed to protect compensated transmission systems in [8]–[10]. In [11], Zonkoly and Desouki introduced a protection algorithm for a shunt-compensated transmission line, based on wavelet entropy. A fault location approach was introduced for a shunt-compensated transmission system, making use of synchronized data, measured from both the ends [12]. Kumar *et al.* [13] developed a protection technique, for the shunt-compensated transmission line, based on synchronized voltages and current signals of both the terminals. A fuzzy logic based distance protection algorithm for transmission line, with STATCOM installed at generator bus, was reported by Raman, *et al.* [14]. Wavelet based protection schemes for transmission line equipped with STATCOM and UPFC had been reported in [15] & [16] respectively. S-transform based distance protection schemes for transmission system, operating with STATCOM, were reported in [1] & [17], [18]. Chanda, *et al.* [19] introduced a scheme for locating fault on a transmission line, making use of wavelet multi-resolution analysis. Wavelet based protection algorithm for transmission line faults, was introduced by Gafoor, *et al.* [20]. The protection schemes, which make use of alienation coefficients of currents recorded on local bus, were presented in [21]. Gafoor *et al.* [22], proposed a protection scheme, making use of wavelet transform (WT) and alienation coefficients of current signals measured at local bus. Protection schemes which make use of wavelet based alienation technique had been proposed by Rathore and Gafoor in [23] & [24]. Costa, *et al.* [25] presented a protection scheme that considered the effect of fault incidence angles. A scheme to locate faults on a transmission line, making use of ANN had been proposed by Tawkif and Morcos in [26]. Purushothama *et al.* [27], had discussed application of ANN approach for estimation of fault location. However there is always a need to investigate the possibility of improving speed of protection by utilizing high speed communication and advanced digital signal processing techniques. The Wavelet transform based algorithm is reported in [15], [16] and [22]. This algorithm can detect the faults in a time duration equal to a half cycle time period.

This paper presents a protection algorithm using wavelet transform, alienation coefficient and artificial neural network

Bhuvnesh Rathore is Assistant Professor with Department of Electrical & Electronics Engineering, MBM Engineering College, Jodhpur-342001, India; email: pg201384006@iitj.ac.in, bbhuvnesh.rathore@gmail.com

Om Prakash Mahela is Assistant Engineer with Power System Planning Division, Rajasthan Rajya Vidyut Prasaran Nigam Ltd., Jaipur-302005, India; e-mail: opmahela@gmail.com

Baseem Khan is Assistant Professor with Department of Electrical and Computer Engineering, Hawassa University, Ethiopia; email: baseem.khan04@gmail.com

H.H. Alhelou is with the Department of Electrical Power Engineering, Tishreen University, 2230 Lattakia, Syria; email: alhelou@tishreen.edu.sy

P. Siano is with the Department of Management & Innovation Systems, University of Salerno, 84084 Salerno, Italy; email: psiano@unisa.it

Manuscript received March 14, 2020.

which can detect, classify and locate the faults, within a quarter cycle time period. The original contribution of the research includes:

- To propose a wavelet-alienation-neural based protection scheme for protection of STATCOM-compensated transmission lines.
- The detection and classification of faults are carried out with the help of wavelet transform and alienation coefficients using quarter cycle data after fault incidence.
- The three phase current signals are utilised to obtain approximate coefficients, further to be used to compute alienation coefficients and fault index for fault analysis.
- Thus, using this approach, fault detection and classification is done in quarter cycle time i.e. 4ms for 60 Hz system.
- Subsequent to fault detection and classification, estimation of fault location is done using quarter cycle based approximate coefficients of current and voltage signals as inputs to ANN.
- The robustness of the algorithm has been proved by testing it with numerous case studies.

The paper is categorized in nine sections. Section two briefs wavelet and alienation techniques and section three demonstrates a wavelet-alienation supported proposed algorithm. Section four presented the utilization of proposed method for the identification and classification of various faults, followed by case studies, covered in section five. Fault location is computed in section six. Performance of algorithm is tested without STATCOM in section seven. Section eight details and advantages and limitation of the algorithm. Section nine concludes the research work.

II. Wavelet and Alienation Techniques

A. Wavelet Transform (WT)

It has a key feature of analysing transients in both frequency and time domain. Signal is divided into low frequency (approximate coefficients) and high frequency (detail coefficients) elements by WT while passing through the filters. The $g(n)$ and $h(n)$ represented the low and high pass filters, respectively. The relationship between these filters is designated as $g(n) = (-1)^n h(1-n)$. WT includes scaling and wavelet functions, defined as follows [24]:

$$\phi(t) = \sqrt{2}\sum h(n)\varphi(2t-n) \tag{1}$$

$$\Psi(t) = \sqrt{2}\sum g(n)\psi(2t-n) \tag{2}$$

Selection of mother wavelets is depended upon its application. For proposed algorithm Daubechies (db-2) is utilized as a mother wavelet. It is selected because performance of algorithm is most efficient for discrimination of the faulty and healthy phases compared to other mother wavelets.

B. Alienation Coefficients

Approximate coefficients based Alienation Coefficients used in this study are computed as follows [24]:

$$A_a = 1 - r_a^2 \tag{3}$$

where, A_a represents Alienation Coefficient and r_a represents correlation coefficient, which is computed as follows [24]:

$$r_a = \frac{N_s(\sum x_a y_a) - (\sum x_a)(\sum y_a)}{\sqrt{[N_s\sum x_a^2 - (\sum x_a)^2][N_s\sum y_a^2 - (\sum y_a)^2]}} \tag{4}$$

where, N_s represents number of samples in a quarter cycle, x_a represents estimated coefficients at t_0 attained from window-W_0. y_a represents estimated coefficients at $(-T+t_0)$ attained from window- W_{-1}, $(T = 16ms)$ as shown in Fig. 1.

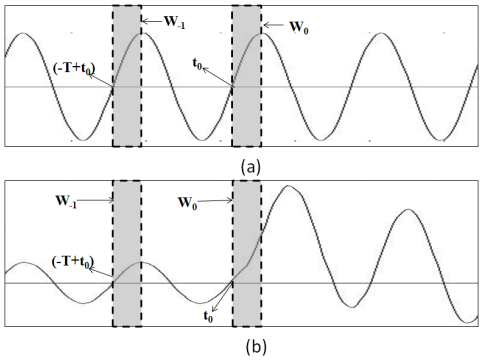

Fig. 1. Comparison windows for computing Alienation Coefficients, (a) during healthy condition, (b) during Fault event at t_0

III. Proposed Algorithm

Fig. 2 presented a block diagram of the system, utilized in this work. The parameters of system [28] are presented in Table I. The AC sources connected to Bus-1 and Bus-2 has an impedance of $Z = 2.9142 + j29.4117\Omega$. STATCOM is realized by 48-pulse IGBT-based converter with 15/500 kV zig-zag transformers rated at 100 MVA. STATCOM is placed at centre of the transmission line with ratings of 500 kV, 60 Hz.

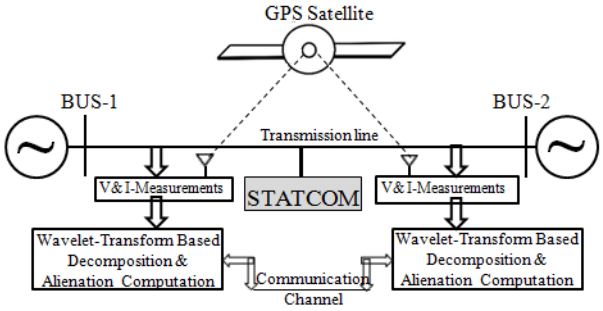

Fig. 2. STATCOM-Compensated Transmission System

Voltage and current waveforms are recorded at both the buses and sampled with a frequency of 1920 Hz. This sampling is synchronized by GPS clock. WT is utilized to analyze current and voltage signals, which are attained over a moving window of width equal to a quarter cycle and approximate coefficients are determined. By comparing the approximate

TABLE I
PARAMETERS OF TRANSMISSION LINE

S. No.	Quantity	Parameters
1	Resistance	$R_0 = 0.3864\Omega/km$, $R_1 = 0.0250\Omega/km$
2	Inductance	$L_0 = 4.1264 \times 10^{-3} H/km$, $L_1 = 9.3370 \times 10^{-4} H/km$
3	Capacitance	$C0 = 7.751 \times 10^{-9} F/km$, $C1 = 12.74 \times 10^{-8} F/km$

coefficients of a current window (W_0) with those of previous window (W_{-1}), at local buses, alienation coefficients are calculated, as described in Fig. 1. Fault Index (FI) is computed as summation of alienation coefficients obtained from local and remote buses. Flow chart illustrating the proposed algorithm is detailed in Fig. 3. All steps used for detecting and classifying the faults are described in this figure. Faults are classified based on number of faulty phases.

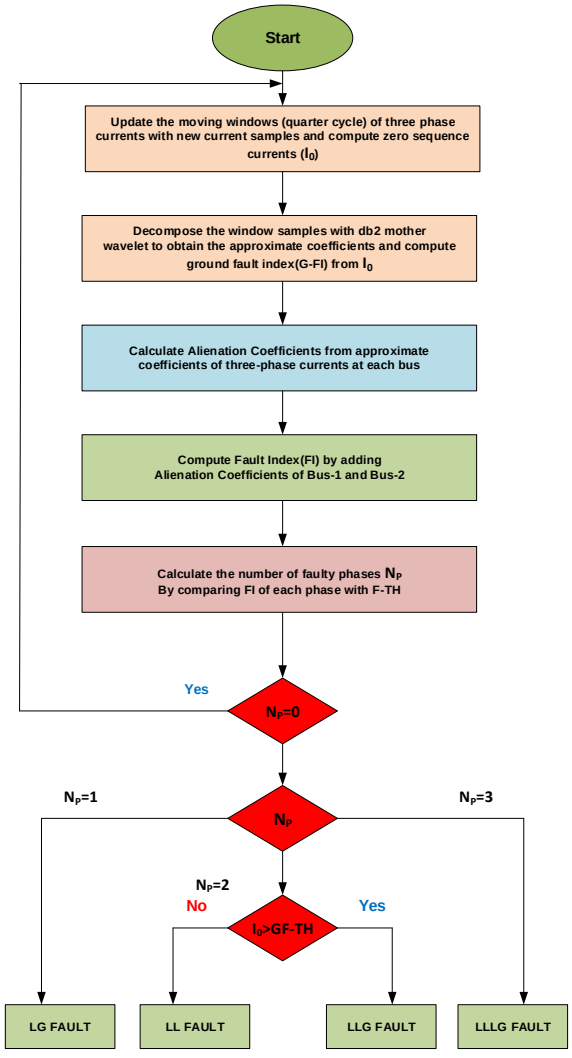

Fig. 3. Flow chart of proposed fault recognition algorithm

Under steady state, the alienation coefficients attained from windows W_0 and W_{-1}, would remain at zero value (and hence the FI) because of their identity. Though, at the time of disturbance, the alienation coefficients would obtain a finite value (and hence the FI), because of the dissimilarities in the signals. This FI is compared with a threshold value (F-TH = 0.2) to detect the fault.

For implementation of proposed algorithm in real world, it will require a computer with high-speed processor and the communication channels among various stations of a power system, which are well established in the modern power system, along with phase measurement units (PMUs), where the sampled signals are synchronized with a GPS clock. Thus, the proposed algorithm does not require any additional infrastructure in the scenario of modern power system.

IV. FAULT DETECTION AND CLASSIFICATION

Figs. 4-5 demonstrate various steps involved in detection of AG fault. Fig. 4(a) and 4(b) show $3-\phi$ current signals measured at bus 1 and bus 2 in respective order. Respective approximate coefficients are detailed in Fig. 4(c) and 4(d). The alienation coefficients, computed over a quarter cycle, based on these approximate coefficients are plotted in Fig. 5(a) and 5(b). Fig. 5(c) illustrates the variation of FI, obtained by adding alienation coefficients of both the buses. It can also be observed that FI of phase-A alone exceeds the threshold value, indicating AG fault.

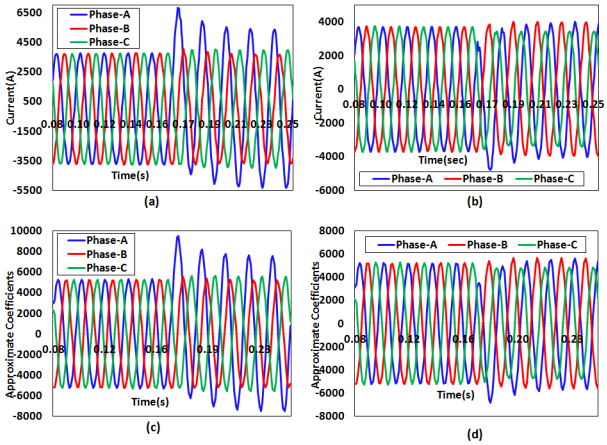

Fig. 4. $3-\phi$ current signals and their approximate coefficients during the event of AG fault, (a) $3-\phi$ Current Signals at bus-1, (b) $3-\phi$ Current Signals at bus-2, (c) Approximate Coefficients of bus-1 current signals, (d) Approximate Coefficients of bus-2 current signals

Fig. 6 presents FI deviation of 3-phases for AB, ABG and ABCG faults. Fig. 6(a) and Fig. 6 (b), show that the FIs of phase-A and B are higher as compared to threshold and therefore it is recognized as two phase fault. It can be observed from Fig. 6(c) that all the 3-phases have FI higher compared to threshold. Thus, it is classified as three-phase fault. However, the differentiation between LL and LLG faults can't be obtained with the developed FI, since the FIs of faulty phases in both the cases demonstrate no apparent differentiation as shown in Fig. 6(a) and 6(b). To differentiate LLG faults from LL faults, a ground fault index (G-FI), which is based on zero sequence current is calculated by summing the approximate decomposition of zero sequence current over a moving window of quarter cycle. This resultant G-FI is

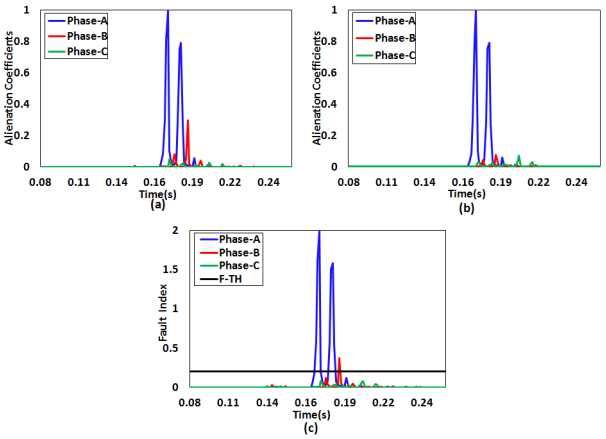

Fig. 5. Detection of AG-fault (a) Alienation Coefficients of approximate coefficients at Bus-1, (b) Alienation Coefficients of approximate coefficients at Bus-2, (c) FI variation with time

TABLE II
PARAMETERS USED FOR VARIATION IN CASE STUDIES

S.No.	Parameters	Range of Variation
1	Fault Location (FL)	0-230km, in steps of 20km, FIA=0°and FIm=0Ω
2	Fault Incidence Angle (FIA)	0°-180°in steps of 30°, FL=40km from bus-1 and FIm=0Ω
3	Fault Impedance (FIm)	0-100Ω, in steps of 20Ω, FL=40km from bus-1 and FIA=0°
4	Noise Contamination	10-100 dB, in steps of 10 dB, FL=40km from bus-1, FIm=0Ω and FIA=0°.
5	Load Switching	10% and 20% load, FL=40km from bus-1, FIm=0Ω and FIA=0°.
6	Sampling Frequency	0.96kHz, 1.92kHz, 3.84kHz and 7.68kHz, FL=40km from bus-1, FIm=0Ω and FIA=0°.
7	STATCOM Control Strategy	VAr Control (Qref. fixed), VAr Control (Iqref. fixed), Voltage Regulation Control, FL=40km from bus-1, FIm=0Ω and FIA=0°
8	STATCOM Location	At the middle of line and at receiving end, FL=40km from bus-1, FIm=0Ω and FIA=0°

compared with a threshold, which is termed as ground fault threshold (GF-TH = 500) for discrimination purpose.

Fig. 6 (d) depicts the G-FI variation for AB and ABG faults. This figure shows that the fault with ground has G-FI greater than the threshold whereas fault without ground has a lower value than the threshold. Thus, for the proposed algorithm the fault detection and classification simultaneously can be done with the help of quarter cycle samples measured just after the fault incidence. Hence, time required to detect and classify fault will be quarter cycle time i.e. (4ms).

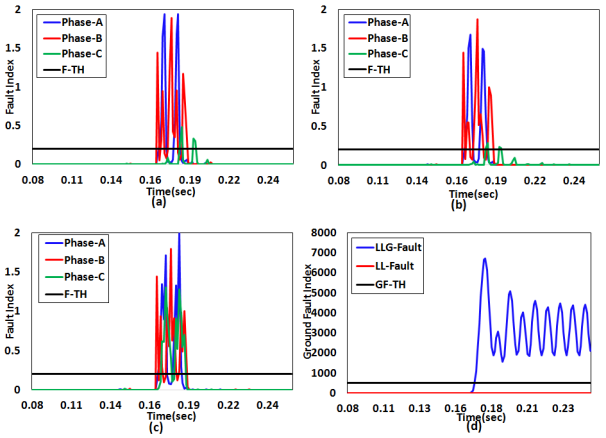

Fig. 6. FI Variation with time, (a) AB Fault, (b) ABG Fault, (c) ABCG Fault, (d) G-FI variation with time

V. CASE STUDIES

For the case study of proposed algorithm, different parameters have been varied and are listed in the Table-II.

A. Effect of Fault Location

Fault locations greatly affect the post fault current transients. Therefore, in this work, the developed algorithm is tested at various fault locations to validate its performance. For this purpose, all types of faults are simulated for every $20km$ along the length of line. Fig. 7 (a) presents the variation of FI with distance for AG fault. From the results it is clear that the value of phase-A FI is greater than the threshold, while for healthy phases (B & C) FI values are lesser than the threshold. It is found that the variation of FIs of phases A and B are always higher as compared to threshold for AB and ABG faults as shown in Fig. 7 (b) and 7 (c), respectively, at all fault locations but the FI of phase-C remains less than the threshold. From Fig. 7 (d), it is evident that the FIs of all phases stay greater than the threshold for ABCG fault at various locations. Therefore, the developed technique is not sensitive to the fault location.

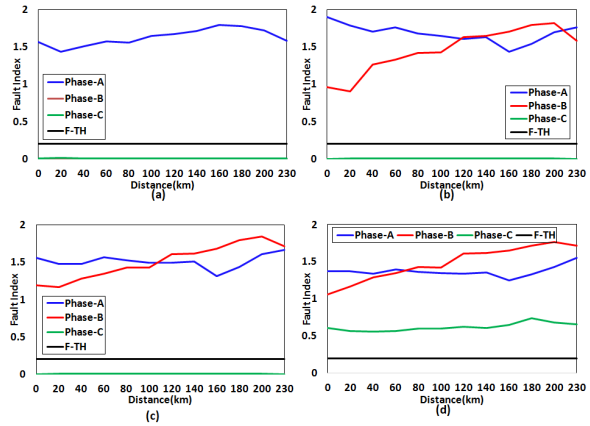

Fig. 7. FI Variation with distance for three phase currents (a) AG Fault (b) AB Fault (c) ABG Fault (d) ABCG Fault

B. Effect of Angle of Fault Incidence

Fault incidence angles greatly affect the value of post fault current transients. Therefore, the developed technique is validated for its effectiveness with variations in fault incidence angle. The range of variation in fault incidence angle is from 0°to 180°in steps of 30°since transients obtained from 180°to 360°are found to be similar to those obtained from 0°to 180°. Fig. 8(a), shows that the FI of only phase-A is higher than

the threshold value, which indicates an AG fault. However, FIs of remaining two phases stays lesser than the threshold. The FI variations of phase A and B, for AB and ABG faults, are presented in Figs. 8(b) and 8(c). From these figures, it is observed that FIs of phase A and B are higher than the threshold irrespective of fault incidence angle. The FIs of all the phases, in case of ABCG fault, remain higher than the threshold value for different incidence angles, as illustrated in Fig. 8(d).

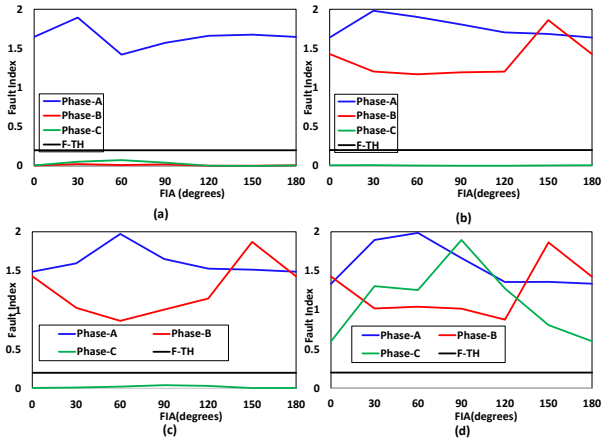

Fig. 8. FI Variation for varying fault incidence angle (FIA) (a) AG Fault (b) AB Fault (c) ABG Fault (d) ABCG Fault

C. Effect of Fault Impedance

In practical power system, during the high impedance faults, sensitivity of the relay reduces due to which the small post-fault currents are not sensed effectively. Therefore, to validate the sensitivity of the developed protection technique with respect to the different fault impedances values, various magnitudes (from 0Ω to 100Ω) of fault impedance are introduced in various types of faults. Fig. 9 illustrates the FI variation for different types of faults, with the variation in fault impedance. Fig 9(a) presents that the FI of phase-A has higher values as compared to the threshold and for other phases, FIs have lower values than the threshold at all the locations, therefore it is detected as AG fault. From Fig. 9 (b) and 9 (c), it is observed that the values of FIs for phase-A and B, are higher than the threshold but for phase-C it is not and therefore, the faults are classified as AB and ABG, respectively. Fig. 9 (d) shows that the index value of all the phases is higher as compared to the threshold; therefore, it is classified as ABCG fault.

D. Effect of Control Strategy of STATCOM

The fault transients also depend on the employed control strategy of STATCOM. Therefore, there is a necessity to validate the developed scheme under different controls of STATCOM operation. Figs. 10(a) and 10(b) present the FI variations for AG and AB faults, respectively, when the STATCOM works under VAr Control (Q_{ref} fixed). It is observed that only faulty phases possess a FI greater than the threshold and other have lower values. Similarly, the Figs. 10(c) and

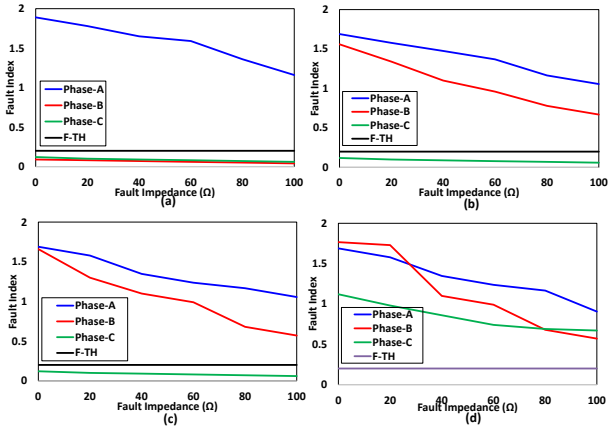

Fig. 9. FI variation for variable fault impedance (a) AG Fault (b) AB Fault (c) ABG Fault (d) ABCG

10(d) illustrate that the FI variations for AG and AB faults when the STATCOM is operating under voltage regulation control. It is seen that the faulty phases have greater FI value than the threshold, whereas the healthy phases have lower value. Thus, it is established that the control mode of STATCOM does not affect the performance of the algorithm.

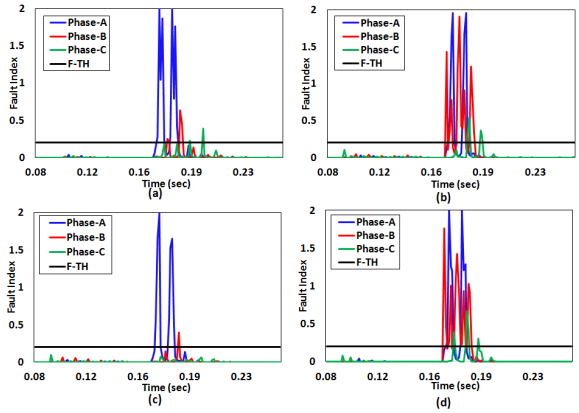

Fig. 10. FI Variation for, (a) AG Fault with Var Control (Qref fixed), (b) AB Fault with Var Control (Qref fixed), (c) AG Fault with Voltage Regulation Control, (d) AB Fault with Voltage Regulation Control

E. Effect of STATCOM location

The location of STATCOM affects the magnitude and transients of bus-currents. Hence, the validation of the developed algorithm is tested by varying the STATCOM location from mid point to receiving end (Bus-2). Figs. 11 (a-d) illustrate the variation of three-phase FI for AG, AB, ABG and ABCG faults, respectively. From these figures, it is observed that the FI of faulty phases exceed the threshold value, whereas those of healthy phases possess a lower value compared to the threshold. Hence, it can be established that the location of STATCOM does not affect the performance of the developed technique.

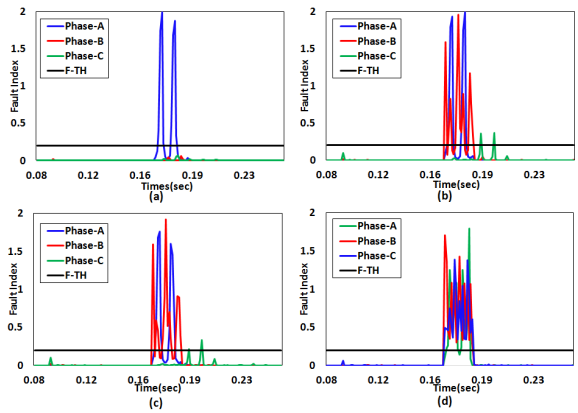

Fig. 11. FI variation for STATCOM installed at bus-2 (a) AG Fault (b) AB Fault (c) ABG Fault (d) ABCG Fault

F. Performance in Noisy Environment

In this work, the current signals are contaminated with different levels of noise for examining the influence of noise on the developed technique. Fig. 12 presents the variation of $3-\phi$ FI for different types of faults, with white Gaussian noise ranging from 10dB SNR to 100dB SNR. Fig 12 (a) presents the variation of FI for AG fault. The FI of phase-A is higher as compared to the threshold and for other phases is lower than the threshold, therefore presented AG fault. Fig 12 (b) and 12 (c) illustrated that FI is higher as compared to the threshold for phase-A and phase-B but not for phase-C, and therefore, the detected faults are AB and ABG faults. Fig. 12 (d) presents that for all the phases, FI is higher than the threshold. Therefore, it is classified as ABCG fault. Therefore, it is clear that the availability of noise in the current signals has no effect on the developed technique.

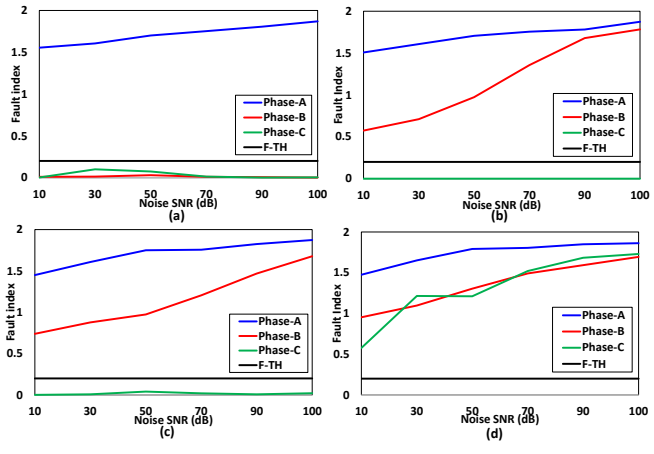

Fig. 12. FI variation for Noisy environment, (a) AG Fault (b) AB Fault (c) ABG Fault (d) ABCG Fault

G. Effect of Loading

The developed technique has been validated with load switching. It has been observed that for 10% and 20% load switching, the maximum values of fault index for phase-A, phase-B and phase-C are 0.04, 0.02 and 0.08, respectively, which are well below the threshold value

H. Effect of Power-Flow Direction

To investigate effect of the direction of power-flow on the proposed algorithm, it has been tested on reverse power flow condition. Since, proposed scheme is making use of data from both the buses, the obtained results corresponding to reverse power flow are same as before.

I. Effect of Sampling Frequency

The algorithm has been tested with sampling frequency of 0.96 kHz, 1.92 kHz, 3.84 kHz and 7.68 kHz; it is observed that increase in frequency has no considerable improvement in terms of accuracy and speed of developed protection scheme. However, reduction in the sampling frequency increases the detection time and error.

VI. Location of Fault

Estimation of location of faults is performed, followed by fault identification and classification, using ANN. Artificial Neural Networks are found to have better pattern recognition capabilities as per the literature survey. Moreover Artificial Neural Networks have following advantages:

- Computation time of the Feed forward neural network is fixed.
- The use of parallel structure has increased the computation speed.
- ANN network is fault tolerant. This is due to the distributed nature of network.
- Network can be programmed in a short time duration for traditional development when explicit mathematical model is not required.
- It is capable to learn from noisy and incomplete data. In this condition, precision of the solution is reduced.
- It can be taught for compensating the changes in system from initial on-line training model.

A multi-layer feed-forward neural network, whose structure is shown in Fig. 13, is used to locate the fault. The details associated with the structure of ANN are provided in Table III. The input is fed from 48 approximate coefficients of $3-\phi$ voltage and current signals of both the ends of the line. Each signal yields 4 approximate coefficients, thus total number of approximate coefficients fed can be given by [2(buses)*(3(phase voltage) + 3(phase current))]*4 = 48 coefficients. The details of simulated data, obtained by a number of case studies are detailed in Table IV. The output of ANN will be fault location (in km) from bus 1. Thus for determination of fault location, the time required is equal to a quarter cycle duration.

Tables V-VI details the performance of algorithm for estimating the fault location using ANN. It can also be inferred that maximum and average errors in locating the faults are

TABLE III
DETAILS OF ANN STRUCTURE

Layer	No. of Neurons	Transfer Function
Input Layer	48	Purelin
Hidden Layer-1	24	Log-sigmoid
Hidden Layer-2	8	Log-sigmoid
Output	1	Purelin

TABLE IV
SIMULATED DATA

S. No.	Attribute	Parameters
1	No. of Fault Locations	24 (for 230 km line, at a steps of 10 kms)
2	Types of Faults	10 (AG, BG, CG, AB, BC, AC, ABG, BCG, ACG, ABCG)
3	Fault Impedances	4 (0, 5,10,15 Ω)
4	Fault Incidence Angle	6 (0, 30, 60, 90, 120, 150)
5	Total number of data sets obtained	24*10*4*6 = 5760
6	ANN Training Data Sets	4032 (70% of total samples)
7	ANN Validation Data Sets	864 (15% of total samples)
8	ANN Testing Data Sets	864 (15% of total samples)

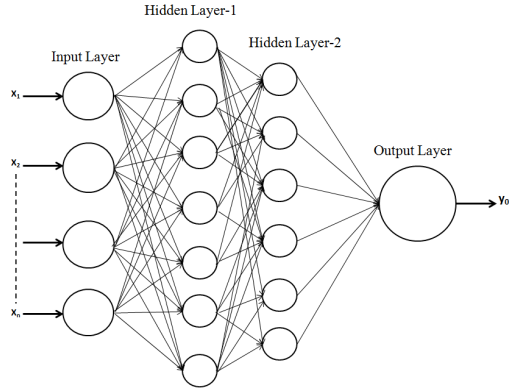

Fig. 13. ANN Structure

2.03% and 0.87% respectively. The error in fault location is computed as follows:

$$Error(\%) = \frac{NNDistance - ActualDistance}{LengthofLine} \times 100 \quad (5)$$

VII. COMPARISON OF PERFORMANCE

In this section, efforts have been made to prove the ability of algorithm to detect and classify the faults, even in the absence of STATCOM (due to maintenance or outage). For this purpose, STATCOM has been disconnected from the transmission line and different types of faults are simulated. Table VII compares the performance of proposed protection scheme with and without STATCOM. From this table, it can be established that the presence and absence of STATCOM device has no effect on algorithm. Table VIII, demonstrates the successful performance of algorithm for BG fault at various locations and with variations in incidence angle. However, due to the space limitation, the results related to demonstration of fully successful performance of the proposed algorithm for CG, BC, AC, BCG, and ACG are not included. A comparative study of algorithm with the algorithms reported in literature is provided in Table IX. It is established that algorithm introduced in this paper is more effective and has high accuracy for fault location compared to the algorithms reported in [29], [28] and [8].

TABLE V
FAULT LOCATIONS RESULTS FOR AG, BG, CG, AB AND BC FAULTS

S.No	Fault type	FIA Fault Imp.	Actual Location	ANN	Location	Error(%)
1	AG	0	0	22	21.07	0.41
2	AG	0	0	143	142.41	0.26
3	AG	0	15	47	49.31	1.00
4	AG	0	15	166	166.39	0.17
5	AG	90	0	87	89.42	1.05
6	AG	90	0	207	209.94	1.28
7	AG	90	15	65	67.22	0.96
8	AG	90	15	135	135.20	0.09
9	BG	0	0	47	46.86	0.06
10	BG	0	0	166	166.64	0.28
11	BG	0	10	65	64.92	0.03
12	BG	0	10	195	194.34	0.29
13	BG	60	0	22	22.02	0.01
14	BG	60	0	135	137.01	0.87
15	BG	60	10	87	90.00	1.30
16	BG	60	10	207	202.11	2.12
17	CG	0	0	65	63.20	0.78
18	CG	0	0	195	197.11	0.92
19	CG	0	5	87	87.32	0.14
20	CG	0	5	207	208.56	0.68
21	CG	120	0	47	44.08	1.27
22	CG	120	0	143	142.96	0.02
23	CG	120	5	22	17.91	1.78
24	CG	120	5	166	169.69	1.60
25	AB	0	0	87	85.59	0.61
26	AB	0	0	207	208.81	0.79
27	AB	0	15	22	21.45	0.24
28	AB	0	15	135	134.36	0.28
29	AB	30	0	65	65.93	0.40
30	AB	30	0	166	167.99	0.87
31	AB	30	15	47	51.73	2.06
32	AB	30	15	143	142.80	0.09
33	BC	0	0	22	21.75	0.11
34	BC	0	0	135	133.87	0.49
35	BC	0	10	47	47.39	0.17
36	BC	0	10	207	201.79	2.27
37	BC	90	0	87	82.30	2.04
38	BC	90	0	195	191.87	1.36
39	BC	90	10	65	62.47	1.10
40	BC	90	10	166	165.58	0.18

VIII. ADVANTAGES AND LIMITATIONS

Advantages and limitations of the proposed protection algorithm are discussed briefly in this section.

A. Advantages

Following are main advantages of the proposed algorithm:

- This algorithm is flexible and can be modified according to system parameters.
- This protection scheme is highly reliable due to the use of data recorded at both ends of line.
- This protection scheme is simplistic in nature and less complex because it is based on comparison of two successive quarter cycle windows of post fault voltages and currents.

TABLE VI
FAULT LOCATIONS RESULTS FOR AC, ABG, BCG, ACG AND ABC FAULTS

S.No	Fault type	FIA Fault Imp.	Actual Location	ANN	Location	Error(%)
1	AC	0	0	47	41.40	2.43
2	AC	0	0	143	147.34	1.89
3	AC	0	5	65	64.48	0.22
4	AC	0	5	195	193.26	0.76
5	AC	120	0	22	22.22	0.10
6	AC	120	0	207	202.05	2.15
7	AC	120	5	87	86.90	0.05
8	AC	120	5	135	136.85	0.81
9	ABG	0	0	65	62.97	0.88
10	ABG	0	0	166	167.99	0.87
11	ABG	0	10	87	85.75	0.54
12	ABG	0	10	135	134.28	0.31
13	ABG	150	0	47	44.48	1.10
14	ABG	150	0	143	142.98	0.01
15	ABG	150	10	22	22.25	0.11
16	ABG	150	10	207	208.44	0.63
17	BCG	0	0	87	86.37	0.27
18	BCG	0	0	195	199.31	1.87
19	BCG	0	5	22	20.06	0.84
20	BCG	0	5	207	200.48	2.83
21	BCG	30	0	65	62.11	1.26
22	BCG	30	0	143	145.91	1.26
23	BCG	30	5	47	46.42	0.25
24	BCG	30	5	166	166.93	0.41
25	ACG	0	0	22	23.42	0.62
26	ACG	0	0	207	210.26	1.42
27	ACG	0	15	47	43.98	1.31
28	ACG	0	15	195	195.26	0.11
29	ACG	90	0	65	64.34	0.29
30	ACG	90	0	166	165.95	0.02
31	ACG	90	15	22	24.67	1.16
32	ACG	90	15	135	139.60	2.00
33	ABC	0	0	47	44.99	0.87
34	ABC	0	0	195	198.32	1.44
35	ABC	0	10	22	20.82	0.51
36	ABC	0	10	207	208.03	0.45
37	ABC	60	0	65	68.20	1.39
38	ABC	60	0	135	131.53	1.51
39	ABC	60	10	87	86.71	0.12
40	ABC	60	10	166	168.77	1.20

TABLE VII
FAULT INDEX VARIATION IN PRESENCE AND ABSENCE OF STATCOM

S.No.	Fault Type	Phase-A		Phase-B		Phase-C	
		Without STAT-COM	With STAT-COM	Without STAT-COM	With STAT-COM	Without STAT-COM	With STAT-COM
1	AG	1.79	1.65	0.01	0.01	0.00	0.01
2	BG	0.12	0.17	1.42	1.47	0.01	0.01
3	CG	0.01	0.01	0.00	0.00	0.90	0.83
4	AB	1.82	1.96	1.48	1.78	0.00	0.01
5	BC	0.00	0.00	1.36	1.42	0.80	0.74
6	AC	1.40	1.19	0.00	0.00	1.00	1.01
7	ABG	1.68	1.72	1.49	1.43	0.00	0.01
8	BCG	0.03	0.05	1.47	1.46	1.10	1.10
9	ACG	1.49	1.30	0.01	0.01	0.97	0.96
10	ABC	1.52	1.33	1.49	1.43	0.63	0.62

- Implementation of proposed protection scheme does not need any extra equipments. Its requires the 3-phase current and voltage measurements which are generally recorded at location of the relays.
- The proposed algorithm makes use of wavelet based approximate decomposition of current signals which has inherent high frequency filtering capability and will take care of the harmonics associated with the CT saturation. Hence, the CT saturation effect is not considered in this study because the proposed algorithm will work well even after CT saturation.
- It was not required to use any feature selection method, as the magnitude of fault current varies inversely with fault impedance or fault location. Moreover deep-learning application requires use of exhaustive processing of data for computation which makes the algorithm and system more complex and costly.

B. Limitations

ANN used for fault location estimation requires exhaustive datasets for training while fault is of random nature. Thus, it is difficult to simulate large number of fault conditions.

IX. CONCLUSION

In this paper, a high speed digital protection scheme, which is effective in detection, classification and location of the fault in a quarter cycle (4ms in case of 60Hz system) is presented, for STATCOM compensated transmission lines. To detect and classify faults, three-phase fault indexes are used, evaluated from approximate decomposition based alienation coefficients of quarter cycle current signals. To estimate fault location, approximate decomposition of three-phase voltages and currents is utilized, to be fed as input to Artificial Neural Network. The average error in fault location is found to be 0.87%. The case studies established that the fault type, fault location, fault incipient angle and fault impedance have no effect on this protection scheme. It has also been proved that the control strategy of STATCOM, its location, load switching, noise contamination and power flow reversal has no effect on proposed algorithm. It is established that algorithm introduced in this paper is more effective, robust and has high accuracy compared to algorithms reported in the literature.

REFERENCES

[1] Y. Gui, C. C. Chung, F. Blaabjerg, and M. G. Taul, "Dynamic extension algorithm based tracking control of statcom via port-controlled hamiltonian system," *IEEE Transactions on Industrial Informatics*, 2019.
[2] W. Zhang, S. Lee, M. Choi, and S. Oda, "Considerations on distance relay setting for transmission line with statcom," in *IEEE PES General Meeting*, July 2010, pp. 1–5.
[3] S. jamali, A. Kazemi, and H. Shateri, "Measured impedance by distance relay for inter phase faults in presence of statcom," in *2008 IEEE Power and Energy Society General Meeting - Conversion and Delivery of Electrical Energy in the 21st Century*, July 2008, pp. 1–6.
[4] G. Li, Y. Chen, A. Luo, and H. Wang, "An enhancing grid stiffness control strategy of statcom/bess for damping sub-synchronous resonance in wind farm connected to weak grid," *IEEE Transactions on Industrial Informatics*, 2019.
[5] X. Liu, L. Che, K. Gao, and Z. Li, "Power system intra-interval operational security under false data injection attacks," *IEEE Transactions on Industrial Informatics*, 2019.
[6] T. S. Sidhu, R. K. Varma, P. K. Gangadharan, F. A. Albasri, and G. R. Ortiz, "Performance of distance relays on shunt-facts compensated transmission lines," *IEEE Transactions on Power Delivery*, vol. 20, no. 3, pp. 1837–1845, July 2005.

TABLE VIII
FAULT INDEX VARIATION FOR BG FAULT

FIA	0			30			60			90			120			150		
Location	A	B	C	A	B	C	A	B	C	A	B	C	A	B	C	A	B	C
20	0.04	1.03	0.01	0.01	1.12	0.18	0.00	1.13	0.17	0.00	1.13	0.12	0.01	1.07	0.02	0.20	0.79	0.01
40	0.08	1.09	0.01	0.01	1.13	0.06	0.00	1.10	0.07	0.00	1.13	0.07	0.07	1.05	0.01	0.18	0.67	0.22
60	0.07	1.29	0.01	0.01	1.11	0.03	0.00	1.11	0.03	0.00	1.11	0.02	0.04	1.08	0.02	0.16	0.68	0.16
80	0.10	1.40	0.01	0.02	1.12	0.03	0.00	1.12	0.01	0.00	1.12	0.01	0.03	1.12	0.04	0.13	0.68	0.11
90	0.17	1.47	0.01	0.01	1.07	0.02	0.00	1.10	0.01	0.00	1.11	0.01	0.08	1.12	0.02	0.14	0.71	0.08
100	0.03	1.56	0.01	0.03	0.90	0.01	0.00	0.99	0.01	0.00	1.01	0.00	0.03	1.11	0.03	0.07	0.76	0.07
120	0.03	1.58	0.00	0.05	0.91	0.03	0.00	0.95	0.01	0.00	0.96	0.00	0.07	1.08	0.03	0.05	0.81	0.07
140	0.01	1.67	0.01	0.07	0.76	0.03	0.00	0.85	0.03	0.00	0.85	0.00	0.08	0.97	0.02	0.18	0.93	0.07
160	0.11	1.64	0.01	0.02	0.68	0.11	0.00	0.72	0.04	0.00	0.74	0.01	0.10	0.84	0.01	0.14	1.05	0.08
180	0.07	1.61	0.01	0.01	0.93	0.25	0.00	0.80	0.09	0.00	0.72	0.01	0.10	0.72	0.00	0.12	1.19	0.13
200	0.11	1.57	0.02	0.08	1.04	0.35	0.00	0.95	0.11	0.00	0.92	0.02	0.18	0.84	0.01	0.15	1.20	0.13
220	0.04	1.03	0.01	0.01	1.12	0.18	0.00	1.13	0.17	0.00	1.13	0.12	0.01	1.07	0.02	0.10	0.79	0.01

TABLE IX
PERFORMANCE EVALUATION AND COMPARATIVE STUDY

Reference	[8]	[28]	[29]	Proposed algorithm
Maximum Error (%)	2.00 (6km)	1.70 (3.91km)	2.52 (5.9km)	2.03 (4.06km)
Average Error (%)	0.53 (1.59km)	1.35 (3.10km)	2.00 (4.6km)	0.87 (2.00km)
Sampling Frequency (Hz)	1k	3.84k	3.84k	1.92k
Effect of Fault Resistance	C	C	C	C
Effect of Fault Incidence Angle	C	C	C	C
Effect of Fault Location	C	C	C	C
Fault Classification	C	C	C	C
Fault Location Estimation	C	C	C	C
Effect of Control Strategy	C	NC	NC	C
Effect of STATCOM location	C	C	C	C
Effect of Noise	NC	NC	NC	C
Effect of Loading	NC	NC	NC	C
Effect of Power Flow Direction	NC	NC	NC	C
Effect of Sampling Frequency	NC	NC	NC	C

*Here, C-Considered and NC-Not Considered

[7] F. A. Albasri, T. S. Sidhu, and R. K. Varma, "Performance comparison of distance protection schemes for shunt-facts compensated transmission lines," *IEEE Transactions on Power Delivery*, vol. 22, no. 4, pp. 2116–2125, Oct 2007.

[8] A. R. Singh, N. R. Patne, V. S. Kale, and P. Khadke, "Digital impedance pilot relaying scheme for statcom compensated tl for fault phase classification with fault location," *IET Generation, Transmission Distribution*, vol. 11, no. 10, pp. 2586–2598, 2017.

[9] M. Tajdinian, M. Allahbakhshi, S. Biswal, O. P. Malik, and D. Behi, "Study of the impact of switching transient over-voltages on ferro-resonance of ccvt in series & shunt compensated power systems," *IEEE Transactions on Industrial Informatics*, 2019.

[10] T. Zeng, X. Ren, and Y. Zhang, "Fixed-time sliding mode control and high-gain nonlinearity compensation for multi-motor driving system," *IEEE Transactions on Industrial Informatics*, 2019.

[11] A. El-Zonkoly and H. Desouki, "Wavelet entropy based algorithm for fault detection and classification in facts compensated transmission line," *International Journal of Electrical Power Energy Systems*, vol. 33, no. 8, pp. 1368 – 1374, 2011.

[12] M. Ghazizadeh-Ahsaee and J. Sadeh, "Accurate fault location algorithm for transmission lines in the presence of shunt-connected flexible ac transmission system devices," *IET Generation, Transmission Distribution*, vol. 6, no. 3, pp. 247–255, March 2012.

[13] B. Kumar, A. Yadav, and A. Y. Abdelaziz, "Synchrophasors assisted protection scheme for the shunt-compensated transmission line," *IET Generation, Transmission Distribution*, vol. 11, no. 13, pp. 3406–3416, 2017.

[14] S. Raman, R. Gokaraju, and A. Jain, "An adaptive fuzzy mho relay for phase backup protection with infeed from statcom," *IEEE Transactions on Power Delivery*, vol. 28, no. 1, pp. 120–128, Jan 2013.

[15] P. V. Rao, S. A. Gafoor, and C. Venkatesh, "Detection of transmission line faults in the presence of statcom using wavelets," in *2011 Annual IEEE India Conference*, Dec 2011, pp. 1–5.

[16] R. K. Goli, A. G. Shaik, and S. T. Ram, "A transient current based double line transmission system protection using fuzzy-wavelet approach in the presence of upfc," *International Journal of Electrical Power Energy Systems*, vol. 70, pp. 91 – 98, 2015.

[17] K. K. R. and P. K. Dash, "A new real-time fast discrete s-transform for cross-differential protection of shunt-compensated power systems," *IEEE Transactions on Power Delivery*, vol. 28, no. 1, pp. 402–410, Jan 2013.

[18] L. Zhou, A. Swain, and A. Ukil, "Reinforcement learning controllers for enhancement of low voltage ride through capability in hybrid power systems," *IEEE Transactions on Industrial Informatics*, 2019.

[19] D. Chanda, N. Kishore, and A. Sinha, "A wavelet multiresolution analysis for location of faults on transmission lines," *International Journal of Electrical Power Energy Systems*, vol. 25, no. 1, pp. 59 – 69, 2003.

[20] S. A. Gafoor and P. V. R. Rao, "Wavelet based fault detection, classification and location in transmission lines," in *2006 IEEE International Power and Energy Conference*, Nov 2006, pp. 114–118.

[21] M. E. Masoud and M. M. A. Mahfouz, "Protection scheme for transmission lines based on alienation coefficients for current signals," *IET Generation, Transmission Distribution*, vol. 4, no. 11, pp. 1236–1244, November 2010.

[22] S. A. Gafoor, S. K. Yadav, P. Prashanth, and T. V. Krishna, "Transmission line protection scheme using wavelet based alienation coefficients," in *2014 IEEE International Conference on Power and Energy (PECon)*, Dec 2014, pp. 32–36.

[23] B. Rathore and A. G. Shaik, "Fault detection and classification on transmission line using wavelet based alienation algorithm," in *2015 IEEE Innovative Smart Grid Technologies - Asia (ISGT ASIA)*, Nov 2015, pp. 1–6.

[24] B. Rathore and A. G. Shaik, "Wavelet-alienation based protection scheme for multi-terminal transmission line," *Electric Power Systems Research*, vol. 161, pp. 8 – 16, 2018.

[25] F. B. Costa, B. A. Souza, and N. S. D. Brito, "Effects of the fault inception angle in fault-induced transients," *IET Generation, Transmission Distribution*, vol. 6, no. 5, pp. 463–471, May 2012.

[26] M. M. Tawfik and M. M. Morcos, "Ann-based techniques for estimating fault location on transmission lines using prony method," *IEEE Transactions on Power Delivery*, vol. 16, no. 2, pp. 219–224, April 2001.

[27] G. Purushothama, A. Narendranath, D. Thukaram, and K. Parthasarathy, "Ann applications in fault locators," *International Journal of Electrical Power Energy Systems*, vol. 23, no. 6, pp. 491 – 506, 2001.

[28] P. K. Dash, S. Das, and J. Moirangthem, "Distance protection of shunt compensated transmission line using a sparse s-transform," *IET Generation, Transmission Distribution*, vol. 9, no. 12, pp. 1264–1274, 2015.

[29] P. Dash, J. Moirangthem, and S. Das, "A new time–frequency approach for distance protection in parallel transmission lines operating with statcom," *International Journal of Electrical Power Energy Systems*, vol. 61, pp. 606 – 619, 2014.